BEST AVAILABLE IMAGES

Defective images within this document are accurate representations of the original documents submitted by the applicant.

Defects in the images may include (but are not limited to):

- BLACK BORDERS
- TEXT CUT OFF AT TOP, BOTTOM OR SIDES
- FADED TEXT
- ILLEGIBLE TEXT
- SKEWED/SLANTED IMAGES
- COLORED PHOTOS
- BLACK OR VERY BLACK AND WHITE DARK PHOTOS
- GRAY SCALE DOCUMENTS

IMAGES ARE BEST AVAILABLE COPY.

As rescanning documents *will not* correct images, please do not report the images to the Image Problem Mailbox.

Radiology

Gabriele A. Krombach, MD
Maythem Saeed, DVM, PhD
Charles B. Higgins, MD
Victor Novikov, MD
Michael F. Wendland, PhD

Index terms:
Animals
Contrast media, experimental studies
Magnetic resonance (MR), contrast media, 511.12143
Myocardium, MR, 511.121411

Published online
10.1148/radiol.2301020228
Radiology 2004; 230:183–190

Abbreviations:
ECG = electrocardiogram
IR = inversion recovery
SE = spin echo

[1] From the Department of Radiology, University of California San Francisco, 505 Parnassus Ave, San Francisco, CA 94143. From the 2001 RSNA scientific assembly. Received March 4, 2002; revision requested May 24; final revision received April 30, 2003; accepted May 20. **Address correspondence to** M.F.W. (e-mail: *mike.wendland@radiology.ucsf.edu*).

Author contributions:
Guarantors of integrity of entire study, M.F.W., G.A.K., M.S., C.B.H.; study concepts, M.F.W., G.A.K., M.S.; study design, M.F.W.; literature research, M.F.W., G.A.K.; experimental studies, G.A.K., M.S., V.N., M.F.W.; data acquisition, G.A.K., M.S., V.N., M.F.W.; data analysis/interpretation, G.A.K., V.N., M.F.W.; statistical analysis, G.A.K., M.F.W.; manuscript preparation, G.A.K., M.F.W.; manuscript definition of intellectual content and editing, G.A.K., M.S., V.N., M.F.W.; manuscript revision/review and final version approval, all authors

Contrast-enhanced MR Delineation of Stunned Myocardium with Administration of $MnCl_2$ in Rats[1]

PURPOSE: To determine whether stunned myocardium can be delineated at magnetic resonance (MR) imaging with differential cellular uptake of manganese ions.

MATERIALS AND METHODS: Twenty-one adult Sprague-Dawley rats underwent either (*a*) a sequence of three episodes of 10 minutes of coronary artery occlusion and 12 minutes of reflow (group 1, $n = 9$); (*b*) a single episode of 10 minutes of occlusion followed by reflow (group 2, $n = 6$), designed to produce different degrees of myocardial stunning; or (*c*) a single episode of 2 minutes of occlusion followed by reperfusion (group 3, $n = 6$), designed to produce no stunning. Ventricular wall thickening was measured on spin-echo (SE) MR images. $MnCl_2$ (0.025 mmol/kg) was intravenously infused for 10 minutes. Highly T1-sensitive inversion-recovery (IR) SE images were obtained to detect subtle regional differences in manganese accumulation. Hearts were stained at sacrifice to define area at risk and to test for myocardial infarction. Significance of differences in mean values was evaluated with repeated-measures analysis of variance.

RESULTS: All hearts were free of infarction, as detected with triphenyltetrazolium chloride staining. On IR SE images, the hearts from rats in groups 1 and 2 exhibited clearly delineated regions of diminished manganese uptake in the expected territory of the occluded artery. The circumferential extent of the manganese-defined defect (45.5% ± 5.6) was similar to that of the area at risk (46.8% ± 7.5). Systolic wall thickening in the defect was significantly ($P < .01$) less than in the nonischemic myocardium (2.7% ± 3.3 vs 31.2% ± 7.5 and 10.0% ± 4.8 vs 28.6% ± 6.5, respectively, for groups 1 and 2). The hearts from rats in group 3 demonstrated no wall thickening deficit or abnormal zone on manganese-enhanced images.

CONCLUSION: Stunned myocardium was delineated with $MnCl_2$-enhanced MR imaging as a hypoenhanced zone. This finding suggests that Ca^{2+} channel activity is diminished in stunned myocardium.

Manganese-based contrast media putatively imparts contrast at magnetic resonance (MR) imaging of the heart according to myocardial cellular function. Mn^{2+} is taken up by myocardial cells through voltage-operated calcium channels and retained for several hours (1,2). Voltage-operated calcium channels are intimately involved in excitation-contraction coupling. Hunter et al (1) showed that agents that increase or decrease myocardial calcium channel activity, such as beta-adrenergic agonists or calcium channel inhibitors, affect manganese uptake in a similar fashion.

These phenomena have also been observed with MR imaging techniques. Vander Elst et al (3) measured manganese uptake and retention in the heart with MR spectroscopy after administering either $MnCl_2$ or mangafodipir (Teslascan; Amersham Health, Princeton, NJ)

and observed diminished uptake when the calcium channel inhibitors verapamil or nifedipine were added. More recently, Hu et al (4) used MR imaging to observe increased manganese-dependent signal enhancement in mice after beta-adrenergic stimulation with dobutamine and inhibition of signal enhancement by adding the calcium channel blocker diltiazem.

In rats that underwent transient regional myocardial ischemia sufficient to produce reperfused infarction, Saeed et al (5) found T1 enhancement in the nonischemic myocardium that remained constant during clearance of manganese from the blood and washout of manganese from the nonfunctional infarcted region. Bremerich et al (6) showed that myocardial infarction could also be delineated at delayed MR imaging after administration of mangafodipir because of differential uptake of Mn^{2+} released from the chelate.

Stunned myocardium is a reversible functional deficit that evolves after a single or repeated brief periods of ischemia (7,8). There are many clinically relevant settings in which stunned myocardium is known to occur, including exercise-induced ischemia, heart transplantation, acute myocardial ischemia, and periinfarction dysfunction (9). The cause of stunned myocardium is thought to involve a combination of transient postreflow calcium overload and oxygen radical damage, which reduces the calcium sensitivity of myofibrils (10). Thus, the stunned myocardium model provides an important experimental setting in which to test the value of manganese-enhanced MR imaging in the evaluation of regional myocardial function.

Accordingly, the purpose of this study was to determine whether stunned myocardium can be delineated at MR imaging with differential cellular uptake of Mn^{2+}.

MATERIALS AND METHODS

$MnCl_2$ Solution

$MnCl_2$ solution was prepared by dissolving crystalline salt (Sigma Chemical, St Louis, Mo) in a 9% saline solution to a final concentration of 25 mmol/L before intravenous infusion at a volume of 1 mL per kilogram of body weight.

Manganese is a paramagnetic divalent cation that has been used as a contrast medium for imaging the heart, liver, and kidneys (11). $MnCl_2$ has a T1 relaxivity of 8 $mmol/L^{-1} \cdot sec^{-1}$ and a T2 relaxivity of 62 $mmol/L^{-1} \cdot sec^{-1}$ in aqueous solution at 40°C and 0.47 T (12). Mn^{2+} has a short plasma half-life of 4.7 minutes (11).

$MnCl_2$, rather than mangafodipir, was used because image contrast evolves quickly after administration due to rapid uptake of free Mn^{2+} by viable heart cells and rapid removal from the blood (1,5); thereafter, image contrast remains unchanged for hours. When mangafodipir is used, Mn^{2+} is released slowly from the chelate (13). The contrast seen on MR images is caused by differential uptake and/or retention of Mn^{2+}, and several hours are required after administration to allow for development of maximal contrast and for clearance from the blood (6). Consequently, it was considered likely that a true short-lived differential uptake of Mn^{2+} would be undetected by using mangafodipir.

Animal Preparation

Care and maintenance of experimental animals were performed in accordance with National Institutes of Heath guidelines. The experimental protocol received prior approval from the committee for animal research at our institution. Surgical procedures were performed by one of two authors (G.A.K. or M.F.W.). Female Sprague-Dawley rats (n = 21, 210–345-g body weight) (Simonsen Laboratories, Gilroy, Calif) were anesthetized with intraperitoneal injection of sodium pentobarbital (50 mg/kg). Additional anesthetic was administered as necessary to maintain inhibition of the corneal reflex. After tracheotomy, the animals received mechanical ventilation at a rate of 60 respirations per minute (Rodent Respirator model 643; Harvard Apparatus, South Natick, Mass). A catheter was placed in a tail vein for delivery of the contrast medium and was used later for infusion of tissue dye. Left thoracotomy was performed at the fourth intercostal space. The left anterior descending coronary artery was occluded by placing a snare ligature around the artery and a small portion of the surrounding myocardium. Reperfusion was accomplished by releasing the ligature.

Rats were divided into three groups. Rats in group 1 (n = 9) underwent a sequence of three episodes of 10 minutes occlusion and 12 minutes reflow to produce stunned myocardium. Rats in group 2 (n = 6) underwent a single episode of 10 minutes occlusion followed by reflow to produce more moderate stunning (10). Rats in group 3 (n = 6) underwent all surgical procedures, but occlusion lasted only 2 minutes and was followed by reperfusion, so as to produce no stunning. Group 3 served as the control group. Myocardial stunning produced with multiple episodes is considered to produce more chronic dysfunction and is reminiscent of dysfunction observed in hibernating myocardium (10).

MR Imaging

MR images were obtained with an MR unit (Omega CSI; Bruker Instruments, Fremont, Calif) at a setting of 2 T. Each animal was placed in the supine position in a home-built birdcage radio-frequency coil and connected to an electrocardiographic (ECG) monitor (Accusync model 61; Advanced Medical Research, Milford, Calif) that provided a continuous readout of heart rate and a trigger signal at the rise of the R wave for prospective cardiac gating of the MR imaging sequences. Heart rate was recorded at approximately 15-minute intervals. For combined respiratory and cardiac gating, a switch was mechanically connected to the ventilator so that it closed during end expiration and passed a 5-V DC signal. The outputs from the ECG trigger and the respiratory switch were connected to a logical AND gate, and ECG trigger pulses were passed to initiate the MR pulse sequence only when the switch was closed. Control of repetition time duration (number of R-R intervals between sequence iterations) and cardiac phase of images was accomplished by placing user-adjustable delay intervals at the beginning and end of the pulse sequence. The animal's core temperature was maintained with a recirculating heated water pad. Imaging commenced a minimum of 30 minutes after final reperfusion.

Coronal and transverse scout images were obtained to guide positioning of the coil to place the heart midventricle at the center of the z gradient and to define the short-axis plane. All MR pulse sequences were carried out with field of view of 50 × 50 mm, matrix of 256 × 128 points zero filled to 256 × 256 points, and section thickness of 2 mm. First, respiratory and ECG-gated spin-echo (SE) short-axis images (repetition time msec/echo time msec, 1,000/12; two excitations) were obtained at two or three adjacent levels of the heart at end systole and end diastole for evaluation of ventricular wall thickening. For end diastolic images, the image data were acquired immediately (14 msec) after the ECG trigger at the rise of the R-wave by setting the predelay interval to 1 msec. End systolic images were

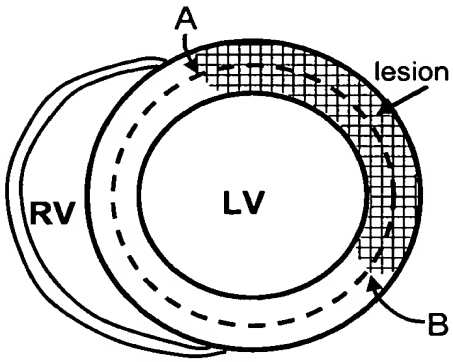

Figure 1. Diagram depicts the method used to measure circumferential extent of the manganese-delineated myocardial defect and of the area at risk defined by blue dye distribution. In this figure, the cylindrical wall—defined by the outer and inner circular solid lines—represents the transverse section of the left ventricle (*LV*). The dashed line inside the circle represents the circumferential midline (centerline) of the left ventricular section. The crosshatched region represents the lesion. The crescent-shaped structure on the left represents the right ventricular (*RV*) free wall. The points labeled *A* and *B* (arrows) indicated on the midline represent the boundary of the lesion along the midline. The circumferential extent of the lesion is defined as the length of the midline between points *A* and *B* within the lesion divided by the length of the entire midline circumference (from *A* to *A*).

acquired by setting the predelay interval to 0.45 of the R-R interval.

$MnCl_2$ (0.025 mmol/kg) was intravenously infused for a 10-minute interval, and conventional T1-weighted ECG-gated images (300/12, four excitations) were obtained before and during the initial 30-minute interval after administration of the contrast medium. At least 30 minutes after administration, respiratory- and ECG-gated inversion-recovery (IR) SE images (repetition time msec/echo time msec/inversion time msec, 1,000–2,000/12/200–400) were obtained to allow the detection of subtle regional T1 differences caused by differential manganese accumulation. For this series of images, a repetition time of 1,000 msec was used. In some animals (two or three per group), a repetition time of 2,000 msec was also used, which has the effect of moderately increasing both the overall signal strength and contrast between regions.

Images were obtained at the same section locations that were acquired for assessment of wall thickening. A nonselective radio-frequency pulse was used for spin inversion. The first three animals in group 1 were used to determine sequence time settings (repetition time and inversion time), at which normal and postischemic regions underwent transition through null signal intensity.

Overall, the MR examination lasted 2½–4 hours for each animal, with 30 minutes spent obtaining systolic and diastolic images, 45 minutes spent obtaining T1-weighted MR images before and after $MnCl_2$ administration, and the remaining time spent obtaining IR SE sequences.

Postmortem Tissue Staining

After MR imaging was completed, the coronary artery was reoccluded, and 0.5 mL of phthalocyanine blue dye suspension at 37°C was administered through the tail vein catheter to demarcate the area at risk (n = 6 for each group). This stain imparts deep blue coloration to perfused myocardium, while the area at risk remains unstained. The heart was excised, and the left ventricle was transversely cut into approximate 2-mm-thick slices. Both surfaces of the slices were imaged with a flatbed scanner (Silverscanner IV; LaCie, Hillsboro, Ore). The slices were then incubated in triphenyltetrazolium chloride solution for 10 minutes at 37°C to test for myocardial infarction. This stain imparts brick red coloration to viable myocardium, while infarcted myocardium remains unstained (14). Hearts from the first three animals in group 1 were stained only with triphenyltetrazolium chloride solution, and slices were examined with a dissecting microscope to carefully scrutinize the myocardium for presence of small foci of infarction.

Data Analysis

Reconstructed images were converted to 8-bit integer format and transferred to a computer (Apple; Macintosh, Cupertino, Calif). Measurements were performed by using public domain image analysis software (NIH Image; National Institutes of Health, available at *rsb.info.nih.gov/nih-image*). Two independent unblinded observers (G.A.K. or M.F.W.) evaluated all images and stained tissue slices, and their findings were averaged together.

IR SE images were evaluated first. If a visually obvious region of abnormal signal intensity along the anterolateral wall was evident on MR images, this region was considered to represent postischemic myocardium. The circumferential extent of this region was measured by tracing a centerline circumferentially through the middle of the myocardial wall and then marking the visually apparent boundary between postischemic and normal myocardium on the centerline (Fig 1). The circumferential extent of the postischemic region was calculated as the length of the centerline within the postischemic zone divided by the entire circumference of the centerline. If postischemic myocardium was not evident on manganese-enhanced MR images (animals in group 3), the postischemic zone was considered to be the typical territory of the occluded vessel, which is the anterolateral wall beginning at the anterior insertion of the right ventricular free wall into the left ventricle and encompassing approximately 40% of the left ventricular circumference. Signal intensities of postischemic and normal myocardium were measured from regions of interest drawn within these respective zones. The regions of interest were drawn to the shape of the myocardial wall and encompassed at least 50% of the visually apparent region on uninterpolated images. The regions of interest chosen on the IR SE images were applied to T1-weighted SE images obtained before and after $MnCl_2$ administration. Signal-to-noise ratio was measured as the mean signal intensity of the region of interest divided by the mean signal intensity within a region of interest of air.

The postischemic boundary markers on IR SE images were applied to SE images obtained at end systole and end diastole to select postischemic myocardium. Wall thickness was measured at four to six evenly spaced circumferential locations within the postischemic myocardium and at six to eight evenly spaced locations within the normal myocardial wall. These respective values were averaged together to obtain a mean wall thickness for normal and postischemic myocardium at end diastole and end systole for each animal. Percentage wall thickening was calculated as the difference between the systolic and diastolic mean wall thicknesses, multiplied by 100, and divided by the diastolic wall thickness.

The circumferential extent of the area defined as at risk on postmortem stained slices was quantified with a centerline procedure similar to that applied to MR images. Both sides of each slice were measured and averaged.

Statistical Analysis

Descriptive statistics and hypothesis testing were accomplished with commer-

cially available statistical software (Statview 5.0; SAS Institute, Cary, NC). All values are shown as mean ± standard error of the mean. Repeated-measures analysis of variance was used to evaluate the significance of mean differences for most measurements (circumferential extent of postischemic myocardium on MR images vs tissue stains, wall thickening, or signal intensity of postischemic vs normal myocardium). If the F score from analysis of variance indicated a significant difference ($P < .05$), the comparison of individual mean differences was evaluated by using the Fisher protected least significant difference test with Bonferroni correction. Differences were considered significant if P was less than .05, per the number of individual comparisons.

RESULTS

The mean heart rate was 365 beats per minute ± 15 at the start of the MR imaging examination and changed very little during 2½ hours of imaging (final heart rate, 357 beats per minute ± 22). Hearts from all animals in groups 1 and 2 exhibited two visually distinct myocardial regions on postcontrast IR SE images (Figs 2, 3; Table 1): normal myocardium, including septal and inferior walls of the heart, and the postischemic myocardium, including the anterior and lateral walls. The best inversion time settings for observing these regions were 200 and 400 msec, which produced approximate null signal for normal myocardium and postischemic myocardium, respectively (Table 1). No animals in group 3 exhibited regional difference in contrast medium accumulation in the left ventricle (Fig 4), and the signal intensity of normal and postischemic myocardium was not significantly different from that of normal regions in animals in groups 1 and 2 (Table 1).

Differential contrast was evident only on IR SE images from animals in group 1 and those in group 2. No differential enhancement was observed on conventional T1-weighted SE images. Instead, a significant increase in MR signal intensity was observed over the entire heart after administering $MnCl_2$ (Fig 5, Table 2), indicating uptake of Mn^{2+} in all myocardial regions.

All animals with a lesion in the postischemic territory on manganese-enhanced images also exhibited less than normal wall thickening in that region (Figs 2 and 3). The mean wall thickening in the postischemic region was significantly less than normal in groups 1 and 2, but not in group 3 (Fig 6). In group 3, animals showed no differential contrast of the postischemic region, and wall thickening along the anterolateral wall was not different from that in the nonischemic regions (Fig 6).

TABLE 1
Signal-to-Noise Ratio of Myocardial Regions on IR SE Images

Inversion Time (msec)	Group 1		Group 2		Group 3	
	Healthy	Injured	Healthy	Injured	Healthy	Injured
200 (n = 3)	2.6 ± 0.9	5.7 ± 0.9	2.0 ± 0.2	4.1 ± 0.3	1.4 ± 0.3	1.3 ± 0.2
400 (n = 6)	4.5 ± 0.4	1.8 ± 0.3*	5.8 ± 0.4	2.0 ± 0.3*	5.1 ± 0.7	4.8 ± 0.6

* $P < .05$ in comparison with healthy myocardial region at repeated-measures analysis of variance performed separately for each group. (No statistical tests were performed for values obtained at an inversion time of 200 msec, because this measurement was performed in only three rats in each group.)

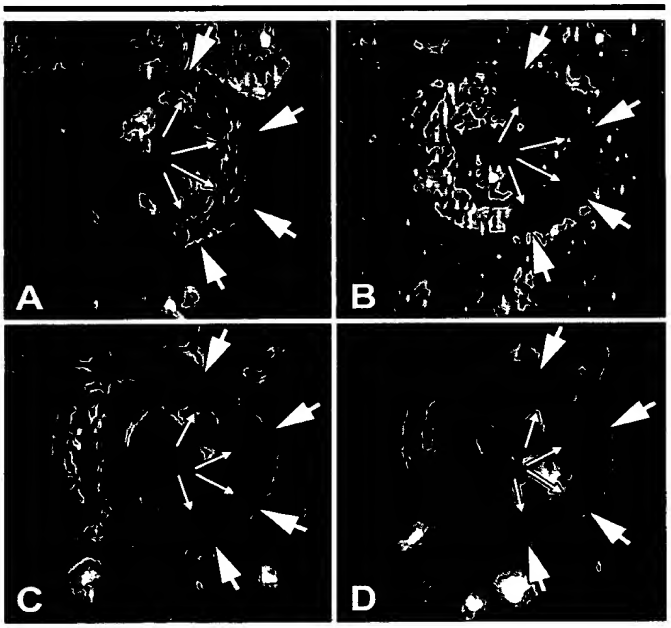

Figure 2. Midventricular SE images obtained in a rat that underwent three sequential 10-minute episodes of left anterior descending coronary artery occlusion and 12 minutes of reflow 1½ hours before administration of 0.025 mmol/kg of $MnCl_2$. All panels are approximately 80 × 80-pixel square inserts cropped from 256 × 256 images, windowed to depict the signal intensity differences, and interpolated once. IR SE images obtained with 1,000/12/200 *(A)*, and 1,000/12/400 *(B)* approximately 45 and 55 minutes, respectively, after administration of $MnCl_2$. SE images (1,000/12) acquired at end diastole *(C)* and end systole *(D)* before administration of $MnCl_2$. In each image, large arrows along the epicardium and small arrows along the endocardium of the anterolateral wall indicate the postischemic zone. *A*, With inversion time of 200 msec, all regions of myocardium had negative signal intensity polarity. Normal myocardium was relatively hypointense since it was approaching null signal, and postischemic myocardium was evident as a hyperintense zone. *B*, With inversion time of 400 msec, all regions of myocardium had positive signal intensity polarity, and postischemic myocardium was relatively hypointense as it emerged from null signal. These contrast patterns indicate that T1 for the postischemic region was longer than for normal myocardium, which indicates that a smaller concentration of Mn^{2+} was present in the postischemic region. In *C* and *D*, the postischemic wall was akinetic, which indicates that the hypoenhanced region was stunned.

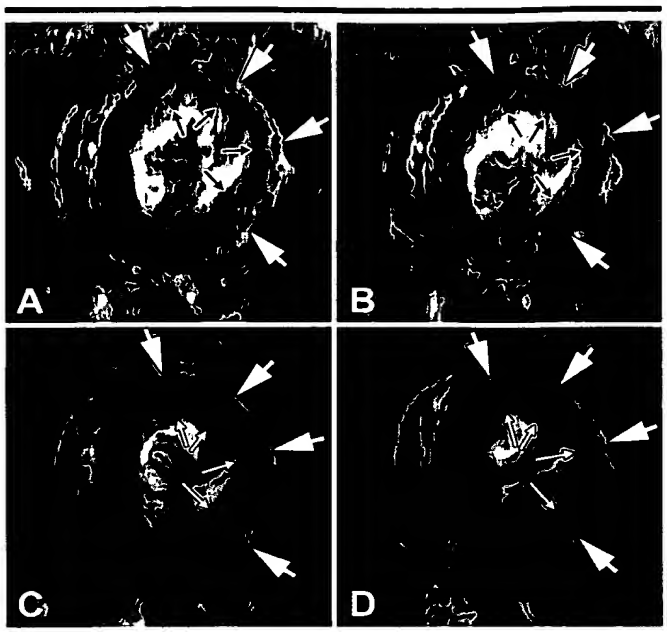

Figure 3. Midventricular SE images obtained in a rat that underwent a single 10-minute episode of left anterior descending coronary artery occlusion followed by reperfusion 2 hours before administration of 0.025 mmol/kg of $MnCl_2$. IR SE images obtained with 2,000/12/200 *(A)* and 2,000/12/400 *(B)* approximately 45 and 95 minutes, respectively, after administration of $MnCl_2$. SE images (1,000/12) acquired at end diastole *(C)* and end systole *(D)*, before administration of $MnCl_2$. In each image, large arrows along the epicardium and small arrows along the endocardium of the anterolateral wall indicate the postischemic zone. Similar to Figure 2, when inversion time was 200 msec, all regions of myocardium had negative signal intensity polarity, and postischemic myocardium was realtively hyperintense in comparison with normal myocardium. When inversion time was 400 msec, all regions of myocardium had positive signal intensity polarity, and postischemic myocardium was relatively hypointense. In *C* and *D*, less than normal wall thickening was evident in the manganese-delineated zone.

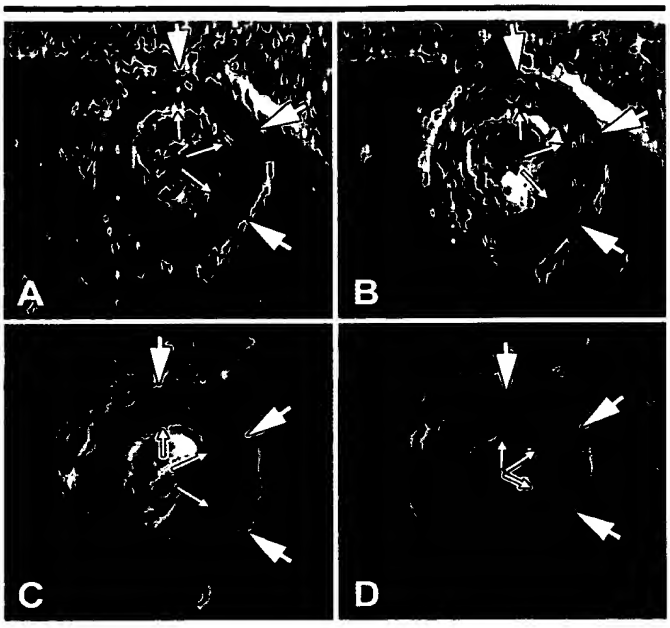

Figure 4. Midventricular SE images obtained in a rat that underwent 2 minutes of left anterior descending coronary artery occlusion followed by reperfusion 1½ hours before administration of 0.025 mmol/kg of $MnCl_2$. IR SE images obtained with 1,000/12/200 *(A)* and 1,000/12/400 *(B)* approximately 40 and 75 minutes, respectively, after administration of $MnCl_2$. SE images (1,000/12) acquired at end diastole *(C)* and end systole *(D)* before administration of $MnCl_2$. In each image, large arrows along the epicardium and small arrows along the endocardium of the anterolateral wall indicate the postischemic zone. *A*, With inversion time set to 200 msec, signal intensity of the entire myocardial wall was uniformly close to null signal, similar to the normal myocardial regions shown in Figures 2 and 3. There was no regional hyperintensity within the postischemic region. *B*, With inversion time of 400 msec, the entire myocardial wall exhibited positive signal intensity polarity, similar to normal myocardial regions in Figures 2 and 3. There was no regional hypointensity in the postischemic region that would signify diminished manganese uptake. In *C* and *D*, normal wall thickening was evident in the postischemic region.

At postmortem examination, no slices of hearts stained with triphenyltetrazolium chloride solution showed evidence of infarction. The area at risk was defined by distribution of blue dye and encompassed a circumferential extent similar to that measured for the region with abnormal manganese accumulation in groups 1 and 2. There was no difference in extent of the area at risk among groups (Fig 7).

DISCUSSION

There were three major findings of our study. First, we found that animals subjected to transient myocardial ischemia designed to produce stunned myocardium showed a lesion of less T1 enhancement compared with normal myocardium after administration of manganese. Second, the defect delineated with Mn^{2+} exhibited less than normal systolic wall thickening, a finding that is consistent with myocardial stunning, and the thickening encompassed the same circumferential extent as the area at risk identified with tissue staining. Third, animals in group 3 that underwent very brief (2 minutes) ischemia exhibited no evidence of stunning and no contrast defect. To our knowledge, these findings show for the first time that stunned myocardium can be delineated as a contrast defect by administering Mn^{2+}, and they suggest a persistent, abnormally low cellular influx of calcium in the dysfunctional region.

Myocardial MR Signal Intensity Changes after $MnCl_2$ Administration

The results of this study showed a significant increase in MR signal intensity over the entire heart on T1-weighted SE images but no discrimination between the postischemic region and normal myocardium. For differential signal intensity to manifest, IR prepared MR imaging was required. There are several potential reasons for this: (*a*) the T1-weighted SE sequence is less sensitive than the IR prepared sequence for discrimination of regions with different T1 values, (*b*) manganese-dependent T2 shortening could have reduced or overridden an otherwise observable T1-dependent signal intensity difference with the T1-weighted SE sequence, and (*c*) repetition time for the T1-weighted sequence may not have been set to provide maximal contrast.

On IR prepared SE images, normal myocardium was hypointense in comparison with postischemic myocardium with inversion time set to 200 msec. Contrast was reversed to hyperintense normal myocardium when inversion time was increased to 400 msec. This result indicates that R1 (1/T1) was greater in

normal versus postischemic myocardium after $MnCl_2$ administration and that substantially more Mn^{2+} was taken up by normal myocardial cells than by postischemic cells. It is not possible, at present, to determine accurately the concentration of Mn^{2+} in either region, because the T1 relaxivity (potency) of manganese will have changed due to complexation of the ion with cellular components such as adenosine triphosphate and proteins.

Figure 5. T1-weighted SE images (400/12) obtained before *(A)* and 30 minutes after *(B)* infusion of 0.025 mmol/kg $MnCl_2$ in a rat that underwent three episodes of 10-minute occlusion followed by 12 minutes of reperfusion. The images were obtained in the same animal as in Figure 2. Uptake of manganese into myocardium was apparent from enhancement of signal intensity in both normal and postischemic myocardium. Large arrows along the epicardial border and small arrows along the endocardial border of the anterolateral wall indicate the postischemic zone. There was very little difference in signal enhancement between normal and postischemic regions on conventional T1-weighted MR images, even though this heart demonstrated a clearly defined hypoenhanced zone on IR SE images.

Relationship between Manganese Uptake and Pathophysiology of Stunned Myocardium

Stunned myocardium is defined as a mechanical dysfunction that persists after reperfusion, despite the absence of irreversible damage and despite restoration of normal or near-normal coronary flow (15). The results of the current study suggest that calcium channel activity is persistently diminished in the stunned myocardium in vivo. This is based on the concept that extracellular Mn^{2+} competes with extracellular Ca^{2+} for binding to and transport through active calcium channels into the myocardial cells during action potential. Accordingly, the quantity of manganese taken up during exposure of the heart to elevated extracellular manganese ion concentration is proportional to the manganese exposure (concentration multiplied by time), the number of active calcium channels, and the calcium influx. The calcium influx triggers the next contraction, and the magnitude of influx regulates the strength of subsequent contractions. Since an intracellular manganese ion does not redistribute (as calcium does), its uptake during the exposure period is stored in the heart cells for many hours.

In the current study, manganese was routinely administered approximately 1½ hours after reperfusion, and the duration of exposure was approximately 15 minutes, including the infusion and roughly 5 minutes of clearance from the blood. Thus, diminished calcium channel activity persisted for at least 1½ hours after reflow. It will be important to determine whether the time course of diminished manganese ion uptake matches the time course of recovery of function.

There are many published reports that describe the mechanism of dysfunction in stunned myocardium, but few have addressed whether calcium channel activity is abnormal. Consequently, there is not a body of literature with which to directly compare this main observation of our study, although a study (16) found diminished calcium channel activity in stunned porcine myocardium. Moreover, the consensus within this field is that the dysfunction is due to primary biochemical damage to intracellular contractile proteins (17) that is caused by a combination of brief calcium overload (18–20) and burst production of damaging oxyradicals (10,21) that are initiated by reperfusion. Key elements supporting this view include findings that intracellular calcium transient is normal in stunned myocardium (19,22) and isolation of damaged proteins from tissue specimens taken from stunned regions (23,24). Within this context, a persistent reduction in calcium influx might be viewed as part of a cellular adaptation to a sublethal injury. It is plausible that reduced calcium influx persists despite a normal intracellular calcium transient as long as calcium efflux by sodium-calcium exchanger is also reduced in compensation (25).

Detection of Dysfunctional Myocardium with MR Imaging

Evaluation of myocardial function with MR imaging and other imaging modalities is performed on the basis of mechanical indices derived from changes in anatomic dimensions (wall motion analysis) or tag locations during the cardiac cycle. These methods are very useful in the detection and characterization of mechanical defects, but they do not provide a means of delineating the injured myocardial tissue that is responsible for the dysfunction. Diminished wall thickening may be produced by a nontransmural tissue injury. Also, the circumferential extent of a mechanical dysfunction may differ from the circumferential extent of the injured tissue that causes it. Moreover, there is currently no known spatial relationship between mechanical dysfunction and the responsible injured myocardial tissue because there has been no method to delineate the injured tissue for direct comparison with mechanical measurements. Thornhill et al (26) reported that gadolinium diethylenetriaminepentaacetic acid is ineffective for distinguishing stunned myocardium from normal myocardium in dogs. Studies of stunned myocardium with positron emission tomography tracers indicate that fluorodeoxyglucose uptake is increased in the dysfunctional zone (27,28). This approach may also provide a method to define dysfunctional myocardium independently from mechanical measurements. With the currently described method to define the dysfunctional tissue as a contrast defect, in combination with image-based mechanical measurements, it may be possible to learn about mechanical consequences of particular local injury patterns.

Manganese-related Cardiotoxicity

It is well known that Mn^{2+} competes with and inhibits cellular uptake of Ca^{2+}. If a sufficiently large concentration of Mn^{2+} is present in the plasma, cardiac arrest will occur due to calcium channel

TABLE 2
Signal-to-Noise Ratio Changes of Myocardial Regions on T1-weighted Images after Administration of $MnCl_2$

Duration of Contrast Medium Administration (min)*	Group 1		Group 2		Group 3	
	Healthy	Injured	Healthy	Injured	Healthy	Injured
Pre	7.6 ± 0.9	7.6 ± 1.0	7.0 ± 0.8	7.4 ± 0.9	7.2 ± 1.5	7.3 ± 2.0
15	13.2 ± 2.0	12.4 ± 1.6	13.1 ± 1.3	15.4 ± 1.5	13.9 ± 1.4	14.1 ± 2.1
20	12.3 ± 2.5	11.5 ± 2.3	13.5 ± 1.4	14.1 ± 2.0	13.0 ± 2.4	13.0 ± 2.6
25	13.7 ± 2.1	12.7 ± 1.8	13.8 ± 1.6	14.9 ± 1.7	12.2 ± 2.4	12.1 ± 2.5
30	13.1 ± 2.8	11.8 ± 2.2	13.5 ± 1.3	13.4 ± 1.9	13.2 ± 2.1	13.1 ± 2.3

* Pre = before administration. $P < .05$ for comparison of precontrast signal-to-noise ratio values with all postcontrast signal-to-noise ratio values at repeated-measures analysis of variance performed separately for each group. There were no significant differences among postcontrast values for each group or between groups at this analysis.

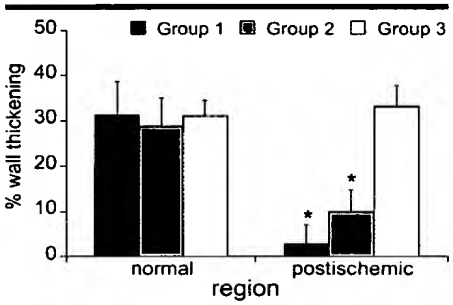

Figure 6. Plot of percentage regional wall thickening (100 multiplied by systolic thickness minus diastolic thickness divided by diastolic thickness) for normal and postischemic myocardium. Rats underwent three episodes of 10-minute left anterior descending coronary artery occlusion and 12 minutes of reflow (group 1), a single 10-minute occlusion (group 2), or a single 2-minute occlusion (group 3). Wall thickening measured in the manganese-delineated postischemic myocardium was significantly reduced compared with that in normal myocardium in animals from groups 1 and 2 prepared for stunned myocardium (* indicates $P < .05$ at repeated-measures analysis of variance). $MnCl_2$ administration failed to delineate postischemic myocardium in the control group (group 3), and there was no significant difference in wall thickening between normal and postischemic myocardium, which indicates absence of myocardial stunning.

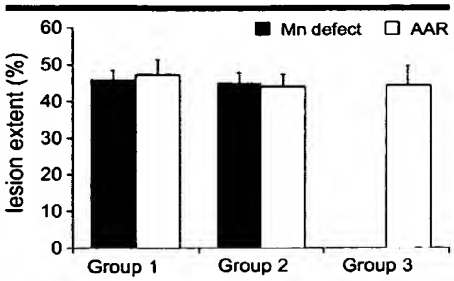

Figure 7. Plot of circumferential extent of postischemic myocardium identified as manganese-delineated defect versus extent of area at risk (*AAR*) defined by exclusion of phthalocyanine blue dye. There was no difference in circumferential extent of area at risk and manganese-delineated defect in two groups of animals prepared for stunning (groups 1 and 2). Animals in the control group (group 3) showed no manganese-delineated defect at MR imaging, yet the area at risk was similar in extent to that of other groups.

blockade. Thus, concern has been raised about cardiotoxicity and the potential for negative inotropic effects (11), both of which have been observed after rapid administration of manganese (29). Cardiac performance was rapidly restored, however, when manganese was removed from the perfusate, despite the fact that myocardium still contained a 60–70-fold higher concentration of Mn^{2+} than normal (29,30).

In another study in dogs prepared with heart failure, no deterioration of cardiac function was observed with slow injection of manganese-based contrast media (31). Moreover, the preponderance of evidence favors the view that acute Mn^{2+} cardiotoxicity is associated primarily with elevated extracellular concentration of the free ion, which inhibits calcium channels, and not with elevated intracellular concentration (30). If this is true, then acute toxicity can be managed by keeping the extracellular concentration of manganese very low, either by slow administration or by administering a chelate complex such as mangafodipir, which releases the ion slowly. With this approach, the fraction of inactive calcium channels is kept at an acceptably low level while Mn^{2+} slowly accumulates in the cells of the heart. It is inescapable, however, that the contrast-producing mechanism in the current application, whether accomplished with slow infusion of Mn^{2+} or with slow release of Mn^{2+} from a chelate, is the loading of an abnormally large concentration of Mn^{2+} into myocardial cells. While administering manganese-chelate formulations may protect heart cells against oxygen toxicity (32), the long-term, potentially deleterious consequences of cellular overload of Mn^{2+} need to be determined. In the current study, we did not observe changes in heart rate or signs of heart failure after slow administration of $MnCl_2$.

Limitations

The current study did not address whether differentiation between stunned and infarcted myocardium is possible after administration of a manganese-based contrast medium. Previous studies (5,6) have shown less than normal manganese accumulation in infarcted myocardium, and it was suggested that this behavior might be useful in delineating viable regions from nonviable ones. The current study shows reduced manganese accumulation in postischemic viable myocardium; therefore, contrast between viable and nonviable injured regions will be reduced, and it is not obvious that these regions will be easily distinguished from each other. This question has to be answered in future experimental studies conducted in animals with small infarction size and surrounding the stunned periinfarction zone.

Practical applications: Results of this study indicate that function-based contrast enhancement can be achieved in the myocardium with delayed contrast-enhanced T1-sensitive MR imaging sequences. This may be particularly valuable in addressing the difficult problem of defining hibernating myocardium. There is substantial evidence that stunned and hibernating myocardium share a common pathophysiology (33). Delineation of hibernating myocardium by means of manganese-based contrast media is therefore promising and should be evaluated in further studies.

Potential toxicity makes it difficult to envision application to humans of a sufficiently high dose of $MnCl_2$ for observable

contrast on MR images; however, delayed imaging performed after slow administration of the clinically approved contrast agent mangafodipir or another manganese-releasing chelate may be possible. Furthermore, manganese 52m positron emission tomography might be used to overcome potential dosage problems when using manganese-based contrast agents for MR imaging, since tracer dosages would be of the order of Mn^{2+} minimum daily dietary requirement (34).

References

1. Hunter DR, Haworth RA, Berkoff HA. Cellular manganese uptake by the isolated perfused rat heart: a probe for the sarcolemma calcium channel. J Mol Cell Cardiol 1981; 13:823–832.
2. Maynard LS, Cotzias GC. The partition of manganese among organs and intracellular organelles of the rat. J Biol Chem 1955; 214:489–495.
3. Vander Elst L, Colet JM, Muller RN. Spectroscopic and metabolic effects of MnCl2 and MnDPDP on the isolated and perfused rat heart. Invest Radiol 1997; 32: 581–588.
4. Hu TC, Pautler RG, MacGowan GA, Koretsky AP. Manganese-enhanced MRI of mouse heart during changes in intropy. Magn Reson Med 2001; 46:884–890.
5. Saeed M, Higgins CB, Geschwind JF, Wendland MF. T1-relaxation kinetics of extracellular, intracellular and intravascular MR contrast agents in normal and acutely reperfused infarcted myocardium using echo-planar MR imaging. Eur Radiol 2000; 10:310–318.
6. Bremerich J, Saeed M, Arheden H, Higgins CB, Wendland MF. Normal and infarcted myocardium: differentiation with cellular uptake of manganese at MR imaging in a rat model. Radiology 2000; 216:524–530.
7. Heyndrickx GR, Millard RW, McRitchie RJ, Maroko PR, Vatner SF. Regional myocardial functional and electrophysiological alterations after brief coronary artery occlusion in conscious dogs. J Clin Invest 1975; 56:978–985.
8. Braunwald E, Kloner RA. The stunned myocardium: prolonged, postischemic ventricular dysfunction. Circulation 1982; 66:1146–1149.
9. Kloner RA, Bolli R, Marban E, Reinlib L, Braunwald E. Medical and cellular implications of stunning, hibernation and preconditioning: an NHLBI workshop. Circulation 1998; 97:1848–1867.
10. Bolli R, Marban E. Molecular and cellular mechanisms of myocardial stunning. Physiol Rev 1999; 79:609–634.
11. Wolf GL, Baum L. Cardiovascular toxicity and tissue proton T1 response to manganese injection in the dog and rabbit. AJR Am J Roentgenol 1983; 141:193–197.
12. Elizondo G, Fretz CJ, Stark DD, et al. Preclinical evaluation of MnDPDP: new paramagnetic hepatobiliary contrast agent for MR imaging. Radiology 1991; 178:73–78.
13. Gallez B, Baudelet C, Adline J, Charbon V, Lambert DM. The uptake of Mn-DPDP by hepatocytes is not mediated by the facilitated transport of pyridoxine. Magn Reson Imaging 1996; 14:1191–1195.
14. Vivaldi MT, Kloner RA, Schoen FJ. Triphenyltetrazolium staining of irreversible ischemic injury following coronary artery occlusion in rats. Am J Pathol 1985; 121: 522–530.
15. Bolli R. Mechanism of myocardial "stunning." Circulation 1990; 82:723–738.
16. Kim SJ, Kudej RK, Yatani A, et al. A novel mechanism for myocardial stunning involving impaired ca(2+) handling. Circ Res 2001; 89:831–837.
17. Mellgren RL, Mericle MT, Lane RD. Proteolysis of the calcium-dependent protease inhibitor by myocardial calcium-dependent protease. Arch Biochem Biophys 1986; 246:233–239.
18. Kusuoka H, Porterfield JK, Weisman HF, Weisfeldt ML, Marban E. Pathophysiology and pathogenesis of stunned myocardium. Depressed Ca2+ activation of contraction as a consequence of reperfusion-induced cellular calcium overload in ferret hearts. J Clin Invest 1987; 79:950–961.
19. Marban E, Kitakaze M, Koretsune Y, Yue DT, Chacko VP, Pike MM. Quantification of [Ca2+]i in perfused hearts: critical evaluation of the 5F-BAPTA and nuclear magnetic resonance method as applied to the study of ischemia and reperfusion. Circ Res 1990; 66:1255–1267.
20. Carrozza JP, Bentivegna LA, Williams CP, Kuntz RE, Grossman W, Morgan JP. Decreased myofilament responsiveness in myocardial stunning follows transient calcium overload during ischemia and reperfusion. Circ Res 1992; 71:1334–1340.
21. Bolli R, Patel BS, Jeroudi MO, Lai EK, McCay PB. Demonstration of free radical generation in "stunned" myocardium of intact dogs with the use of the spin trap alpha-phenyl N-tert-butyl nitrone. J Clin Invest 1988; 82:476–485.
22. Gao WD, Atar D, Backx PH, Marban E. Relationship between intracellular calcium and contractile force in stunned myocardium: direct evidence for decreased myofilament Ca2+ responsiveness and altered diastolic function in intact ventricular muscle. Circ Res 1995; 76:1036–1048.
23. Gao WD, Liu Y, Mellgren R, Marban E. Intrinsic myofilament alterations underlying the decreased contractility of stunned myocardium: a consequence of Ca2+-dependent proteolysis? Circ Res 1996; 78:455–465.
24. Gao WD, Atar D, Liu Y, Perez NG, Murphy AM, Marban E. Role of troponin I proteolysis in the pathogenesis of stunned myocardium. Circ Res 1997; 80: 393–399.
25. Eisner DA, Trafford AW, Diaz ME, Overend CL, O'Neill SC. The control of Ca release from the cardiac sarcoplasmic reticulum: regulation versus autoregulation. Cardiovasc Res 1998; 38:589–604.
26. Thornhill EE, Prato FS, Pereira RS, Wisenberg G, Sykes J. Examining a canine model of stunned myocardium with Gd-DTPA-enhanced MRI. Magn Reson Med 2001; 45:864–871.
27. Fallavollita JA, Canty JM Jr. Differential 18F-2-deoxyglucose uptake in viable dysfunctional myocardium with normal resting perfusion: evidence for chronic stunning in pigs. Circulation 1999; 99: 2798–2805.
28. Camici PG, Dutka DP. Repetitive stunning, hibernation, and heart failure: contribution of PET to establishing a link. Am J Physiol Heart Circ Physiol 2001; 280:H929–H936.
29. Brurok H, Schojtt J, Berg K, Karlsson JO, Jynge P. Effects of manganese dipyridoxyl diphosphate, dipyridoxyl diphosphate–, and manganese chloride on cardiac function: an experimental study in the Langendorff perfused rat heart. Invest Radiol 1995; 30:159–167.
30. Brurok H, Schjott J, Berg K, Karlsson JO, Jynge P. Manganese and the heart: acute cardiodepression and myocardial accumulation of manganese. Acta Physiol Scand 1997; 159:33–40.
31. Karlsson JO, Mortensen E, Pedersen HK, Sager G, Refsum H. Cardiovascular effects of MnDPDP and MnCl2 in dogs with acute ischaemic heart failure. Acta Radiol 1997; 38:750–758.
32. Brurok H, Ardenkjaer-Larsen JH, Hansson G, et al. Manganese dipyridoxyl diphosphate: MRI contrast agent with antioxidative and cardioprotective properties? Biochem Biophys Res Commun 1999; 254:768–772.
33. Shen YT, Vatner SF. Mechanism of impaired myocardial function during progressive coronary stenosis in conscious pigs: Hibernation versus stunning? Circ Res 1995; 76:479–488.
34. Atkins HL, Som P, Fairchild RG, et al. Myocardial positron tomography with manganese-52m. Radiology 1979; 133:769–774.